

AD-A165 277

CONCEPT STUDY OF A MULTIPLE BEAM LENS ANTENNA WITH AN
INTERNAL PHASE SHIFT MASK(U) ROME AIR DEVELOPMENT
CENTER GRIFFISS AFB NY D T MCGRATH AUG 85

1/1

UNCLASSIFIED

RADC-TR-85-159

F/G 9/5

NL

			END										
			FILED										
			DTIC										



MICROCOPY RESOLUTION TEST CHART
NATIONAL BUREAU OF STANDARDS-1963-A

(11)

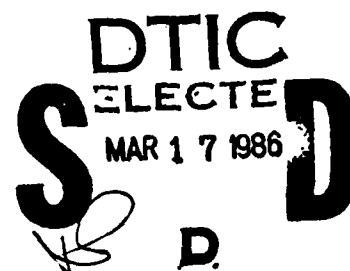
AD-A165 277

RADC-TR-85-159
In-House Report
August 1985



**CONCEPT STUDY OF A MULTIPLE BEAM
LENS ANTENNA WITH AN INTERNAL
PHASE SHIFT MASK**

Daniel T. McGrath, Captain, USAF



APPROVED FOR PUBLIC RELEASE; DISTRIBUTION UNLIMITED

DTIC FILE COPY

ROME AIR DEVELOPMENT CENTER
Air Force Systems Command
Griffiss Air Force Base, NY 13441-5700

86 3 17 161

This report has been reviewed by the RADC Public Affairs Office (PA) and is releasable to the National Technical Information Service (NTIS). At NTIS it will be releasable to the general public, including foreign nations.

RADC-TR-85-159 has been reviewed and is approved for publication.

APPROVED:



PAUL H. CARR, Acting Chief
Antennas & RF Components Branch
Electromagnetic Sciences Division

APPROVED:



ALLAN C. SCHELL
Chief, Electromagnetic Sciences Division

FOR THE COMMANDER:



JOHN A. RITZ
Plans Office

If your address has changed or if you wish to be removed from the RADC mailing list, or if the addressee is no longer employed by your organization, please notify RADC (EEA) Hanscom AFB MA 01731. This will assist us in maintaining a current mailing list.

Do not return copies of this report unless contractual obligations or notices on a specific document requires that it be returned.

Unclassified

SECURITY CLASSIFICATION OF THIS PAGE

REPORT DOCUMENTATION PAGE				
1a. REPORT SECURITY CLASSIFICATION Unclassified		1b. RESTRICTIVE MARKINGS		
2a. SECURITY CLASSIFICATION AUTHORITY		3. DISTRIBUTION/AVAILABILITY OF REPORT Approved for public release; distribution unlimited		
2b. DECLASSIFICATION/DOWNGRADING SCHEDULE				
4. PERFORMING ORGANIZATION REPORT NUMBER(S) RADC-TR-85-159		5. MONITORING ORGANIZATION REPORT NUMBER(S)		
6a. NAME OF PERFORMING ORGANIZATION Rome Air Development Center		6b. OFFICE SYMBOL (If applicable) RADC/EEAA		7a. NAME OF MONITORING ORGANIZATION
6c. ADDRESS (City, State and ZIP Code) Hanscom AFB Massachusetts 01731		7b. ADDRESS (City, State and ZIP Code)		
8a. NAME OF FUNDING/SPONSORING ORGANIZATION		8b. OFFICE SYMBOL (If applicable)		9. PROCUREMENT INSTRUMENT IDENTIFICATION NUMBER
8c. ADDRESS (City, State and ZIP Code)		10. SOURCE OF FUNDING NOS.		
		PROGRAM ELEMENT NO. 62702F	PROJECT NO. 4600	TASK NO. 14
				WORK UNIT NO. 01
11. TITLE (Include Security Classification) Concept Study of a Multiple Beam Lens Antenna With an Internal Phase Shift Mask				
12. PERSONAL AUTHOR(S) Daniel T. McGrath, Capt, USAF				
13a. TYPE OF REPORT In-House		13b. TIME COVERED FROM _____ TO _____		14. DATE OF REPORT (Yr., Mo., Day) 1985 August
15. PAGE COUNT				
16. SUPPLEMENTARY NOTATION				
17. COSATI CODES			18. SUBJECT TERMS (Continue on reverse if necessary and identify by block number)	
FIELD	GROUP	SUB. GR.		
09	03		Microwave lens, Electronically-scanned antenna, Lens antennas, Satellite communications Multiple-beam antennas.	
19. ABSTRACT (Continue on reverse if necessary and identify by block number)				
<p>A new antenna architecture has been investigated to assess its usefulness for limited scan systems. It consists of a passive lens with a few small subarrays spaced evenly across its focal surface. Between the lens and the focal surface is a phase shift layer, or "mask", comprised of oppositely-facing planar arrays interconnected by phase shifters (similar to a phased array lens). The mask redirects a focusing wave from an arbitrary angle onto one of the subarrays.</p> <p>It is shown that a system with only 19 small subarrays, and a mask containing about 4500 elements could provide complete earth coverage with as many as 19 simultaneous 0.3° beams. The pattern quality of those beams is good, provided that no two are steered to within a few beamwidths of each other.</p>				
20. DISTRIBUTION/AVAILABILITY OF ABSTRACT UNCLASSIFIED/UNLIMITED <input type="checkbox"/> SAME AS RPT. <input checked="" type="checkbox"/> DTIC USERS <input type="checkbox"/>			21. ABSTRACT SECURITY CLASSIFICATION Unclassified	
22a. NAME OF RESPONSIBLE INDIVIDUAL Daniel T. McGrath, Capt, USAF			22b. TELEPHONE NUMBER (Include Area Code) (617) 861-4036	22c. OFFICE SYMBOL RADC/EEAA

DD FORM 1473, 83 APR

EDITION OF 1 JAN 73 IS OBSOLETE.

Unclassified

SECURITY CLASSIFICATION OF THIS PAGE

Contents

1. INTRODUCTION	1
2. THE SYSTEM CONCEPT	2
3. LIMITED SCAN SYSTEM	2
3.1 Beamforming Lens	4
3.2 Subarrays	8
3.3 Grating Lobe Analysis	8
4. SCANNING CHARACTERISTICS	13
4.1 Beam Steering Algorithm	13
4.2 Single Beam Scanning	15
4.3 Multiple Beam Scanning	15
5. CONCLUSIONS	23

Illustrations

1. Generalized Concept	3
2. Limited Scan System	3
3. Effects of Scanning Aberrations With a One Degree of Freedom Lens	5
4. Geometry of a Two Degree of Freedom Lens	6
5. Scanned Beam Patterns of a Two Degree of Freedom Lens	7

Illustrations

6. Synthesized Low Sidelobe Patterns Using a Three-Element Feed, $F = L = 200\lambda$	9
7. Reference Geometry for Grating Lobe Analysis	10
8. Maximum Lens Element Spacing vs Mask Position	10
9. Maximum Mask Element Spacing vs Mask Position	11
10. Number of Mask Elements Required for a 233λ Aperture	12
11. Reference Geometry for Beam Steering	13
12. Scanned Subarray Patterns, $\alpha_0 = 6^\circ$, $F = L = 200\lambda$	14
13. Oblique Mask Illumination by the Subarray, 6° Subarray Scanned to 9°	16
14. Percentage Mask Overlap by Adjacent Subarrays	17
15. Effect on 6° Subarray's Pattern Due to Scanning of 0° Subarray, $F = L = 200\lambda$, 7-Element Subarray	18
16. Scanned Patterns of 6° Subarray With 0° Subarray Unscanned, $F = L = 200\lambda$, 7-Element Subarray	20
17. Scanned Patterns With Long Focal Length, $F = 2L = 400\lambda$, $D = F/8$	21
18. Scanned Patterns With Short Focal Length and Smaller Subarray Spacing, $F = L = 200\lambda$, $D = F/16$	22

Concept Study of a Multiple Beam Lens Antenna With an Internal Phase Shift Mask

1. INTRODUCTION

Because of the proliferation of users of satellite communications antennas, and the decreasing number of available orbital slots, fixed-beam antennas are becoming less attractive. Current emphasis is shifting toward antennas with multiple, independent, retargetable beams. Phased arrays prove too expensive because they require a separate set of phase shifters and a separate corporate feed network for each beam. Conventional lens or reflector concepts are also undesirable because the focal array will contain an extremely large number of elements, with a separate feed network for each of many fixed beams, or a large switching matrix to access all possible beam locations. In any case, phased array or reflector or lens, the number of control elements is too high, and the antenna too expensive.

Mailloux¹ has proposed a multibeam antenna design that may solve this dilemma. It is comprised of a passive beamforming lens with a small number of subarrays on its focal surface. Between the lens and focal surface is a layer similar to a phased-array lens, antenna elements on both surfaces interconnected by phase shift modules, which steers a focusing wave from the lens to the nearest subarray. This report shows that such an antenna will be capable of forming simultaneous, low sidelobe

(Received for publication 27 August 1985)

1. Mailloux, R. J. patent disclosure.

1

Accession For	
NTIS	CRA&I <input checked="" type="checkbox"/>
DTIC	TAB <input type="checkbox"/>
Unannounced <input type="checkbox"/>	
Justification	
By	
Distribution /	
Availability Codes	
Dist	Avail and/or Special
A-1	

beams within non-overlapping sectors. The required number of control elements is far fewer than would be required for a phased array with the same number of beams.

Although the system concept as proposed by Mailloux¹ is much more general, we have chosen to apply it to the problem of a receive-only communications satellite in geosynchronous orbit. We will ultimately show that in that application, an antenna with nineteen very small subarrays can provide complete earth coverage with very fine angular resolution. Provided that no two users are within a few beamwidths of each other, low sidelobes can be maintained.

2. THE SYSTEM CONCEPT

The basic concept is depicted in Figure 1. A constrained, or "bootlace" lens focuses an incident plane wave onto the focal arc. Ordinarily, scanning a given angular region would require that the focal arc be completely populated with receiving elements at intervals of a lens beamwidth. But in this case, the phase shift layer captures the converging spherical wave and redirects it to one of a small number of "subarrays." Since the phase shift layer does no focusing, we will refer to it as the "mask" to distinguish it from similar lens structures that are used for focusing as well as beam steering (phased array lenses).

As the converging waves from sources at different locations in angle approach the focal arc, they become more and more separated. Provided they do not overlap too much on the mask, they can be steered to the nearest subarray without significant degradation in pattern quality. But no matter how close the mask is to the focal arc, there will always be some overlap when the far-field sources are near enough in angle. Thus, the immediate question is what the practical limits are on the angular separation of the independent beams. Those limits will determine the extent of the coverage regions, and the number of users that can be served simultaneously.

3. LIMITED SCAN SYSTEM

The system we have chosen to simulate is depicted in Figure 2. The passive lens, whose aperture width is L , focuses a wave from the far field onto a focal arc of radius F . The steering mask is located a distance D from the center of the focal arc.

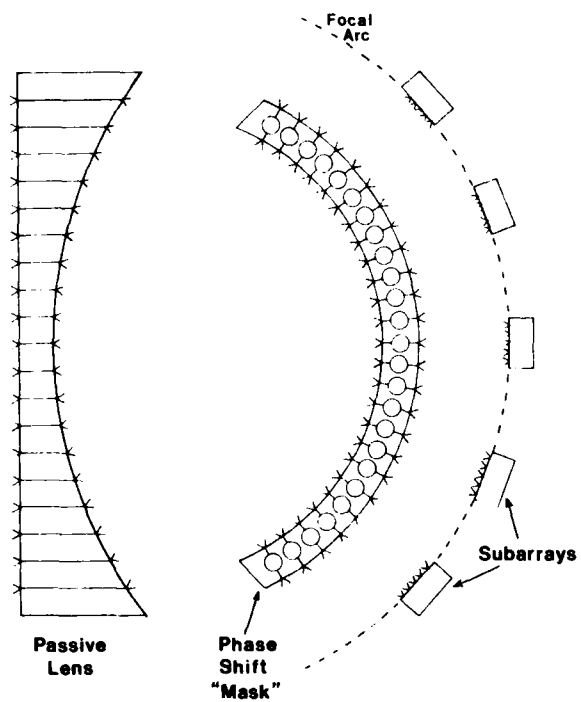


Figure 1. Generalized Concept

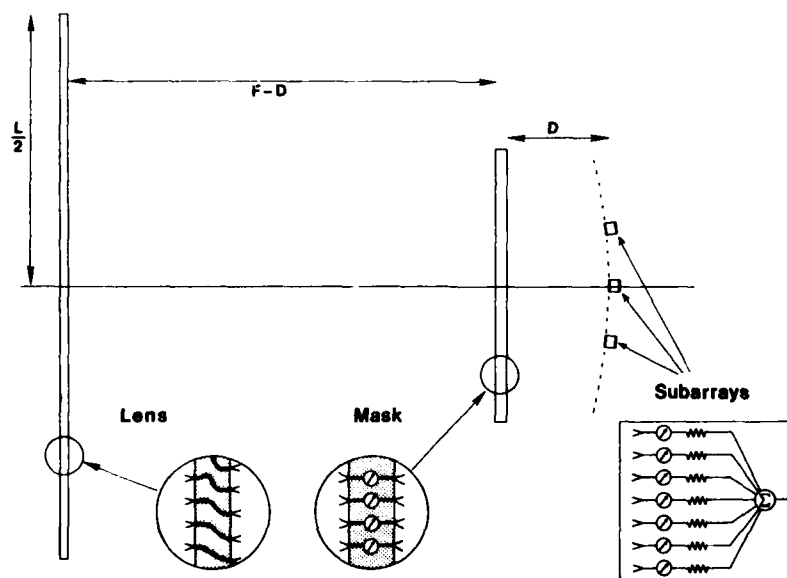


Figure 2. Limited Scan System

At geosynchronous altitude, the earth subtends a solid angle of 17° . We would typically design for 18° to allow for platform boresight error. To cover 18° in one plane only, three subarrays are positioned at -6° , 0° and $+6^\circ$ on the focal arc. Those are the nominal scan angles α_1 , α_2 and α_3 . Each subarray will scan $\pm 3^\circ$ about its nominal scan angle.

This section deals with "system" issues: the lens design; the subarray design; and the required number and spacing of elements in the lens, mask and subarrays that will prevent grating lobe effects.

3.1 Beamforming Lens

We initially considered the simplest type of constrained lens as a beamformer. Radiating elements on opposing faces are joined by transmission lines whose lengths are longest in the center and shortest at the edges:

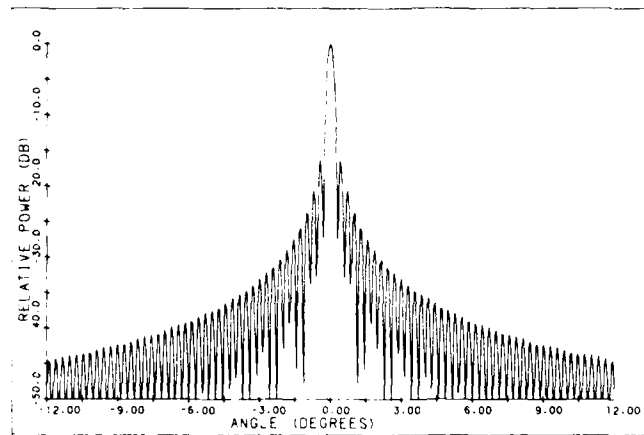
$$W(y) = W_0 + F - [F^2 + y^2]^{1/2} \quad (1)$$

However, such a lens is not capable of forming quality beams over more than a few beamwidths off its boresight axis. Figure 3 illustrates the progressive degradation as a single feed element is moved along the focal arc from 0° (Figure 3a) to 2.5° (Figure 3b) and 5° (Figure 3c). This simulation used sample parameters of $F = L = 200\lambda$ with 3.4λ spacing between lens elements. The severe coma (third order) aberrations of this lens would therefore prevent a small subarray at no more than 2.5° from the lens axis from synthesizing a low sidelobe pattern.

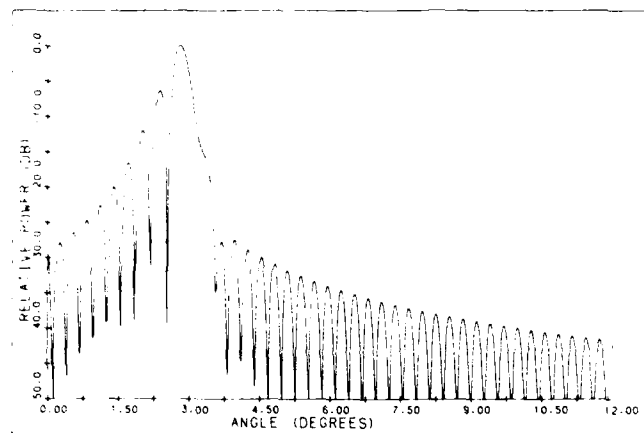
There are a number of multifocal beamformer designs that are certainly capable of scanning a low sidelobe beam over the required $\pm 9^\circ$. However, from the standpoint of a three-dimensional lens, that is, for scanning in azimuth and elevation, they are undesirable because at least one of the faces must be curved, making fabrication difficult. If instead, both lens faces are flat, but the feed side elements are displaced, as shown in Figure 4, the focusing is near-perfect over at least $\pm 12.5^\circ$. Complete details of this lens design are given in Reference 2. The position y of a back face element in terms of the position η of its corresponding front face element is

$$y = \eta \left[\frac{F^2 - \eta^2 \sin^2 \beta}{F^2 - \eta^2} \right]^{1/2} \quad (2)$$

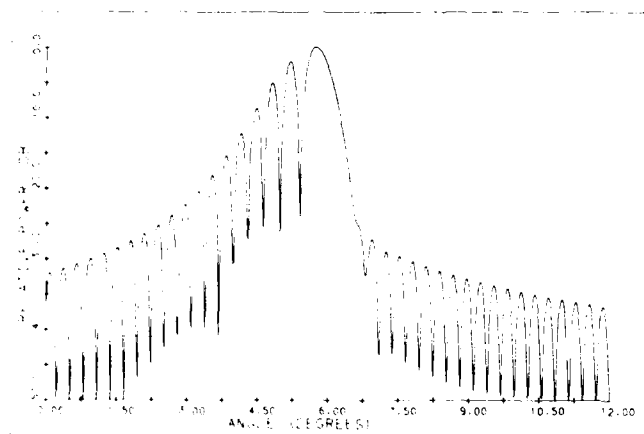
2. McGrath, D. T. (1985) Two Degree of Freedom Linear and Planar Microwave Array Lenses, RADC-TR-84-215, AD A153701.



(a)



(b)



(c)

Figure 3. Effects of Scanning Aberrations With a One Degree of Freedom Lens: (a) On-axis Beam Pattern, (b) Scanned Beam, and (c) 6.0° scanned Beam

where β is the off-axis angle of the two perfect focal points. The pair of elements at y and η are joined by a transmission line of length

$$W = W_0 + F - 0.5[F^2 + y^2 - 2yF \sin \beta]^{1/2} - 0.5[F^2 + y^2 + 2yF \sin \beta]^{1/2} \quad (3)$$

where W_0 is an arbitrary constant. Beam patterns for this lens, again with $F = L = 200\lambda$, are Figures 5a and 5b ($\beta = 0^\circ$). Note that the first sidelobes of these beams are not at -12 dB as one would expect for a uniform aperture illumination because of the cosine patterns of feed and lens elements.

Notice that there is some deterioration in the main beam region of Figure 5b, caused by quadratic phase error. That "focus" aberration is corrected by moving the feed closer to the lens center. The optimum distance G of the feed from the lens center is a function of angle:

$$G(\alpha) = \frac{F}{\cos \beta} \left[1 + 0.5 \frac{\sin^2 z \sin^2 \alpha}{[1 - \sec z][1 + \sin z \sin \alpha]} \right] \quad (4a)$$

$$z = \sin^{-1}(L/2F) \quad (4b)$$

resulting in the improved beam pattern of Figure 5c.

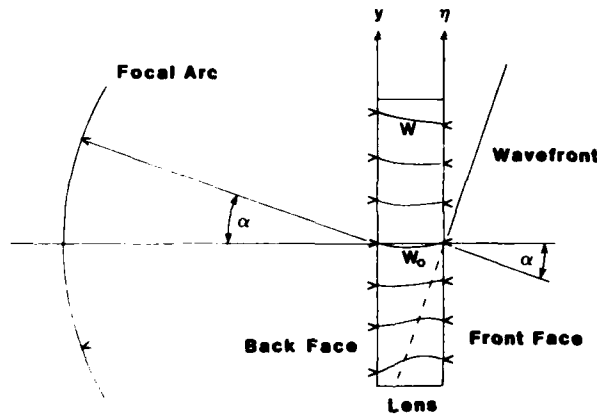
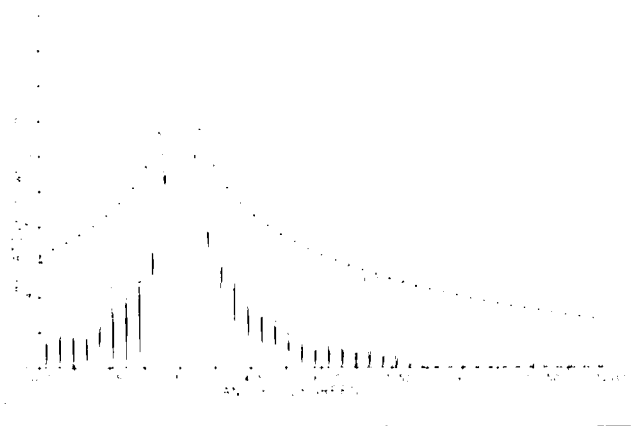
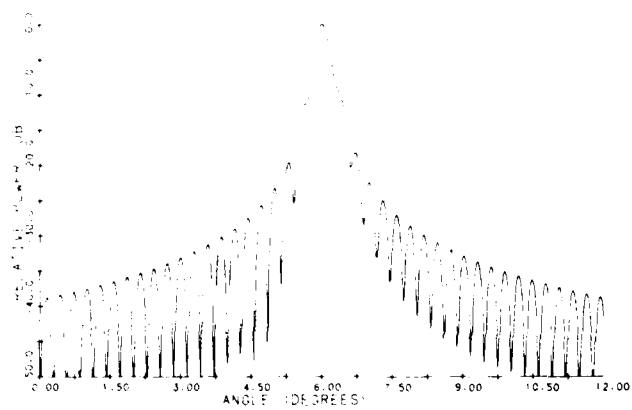


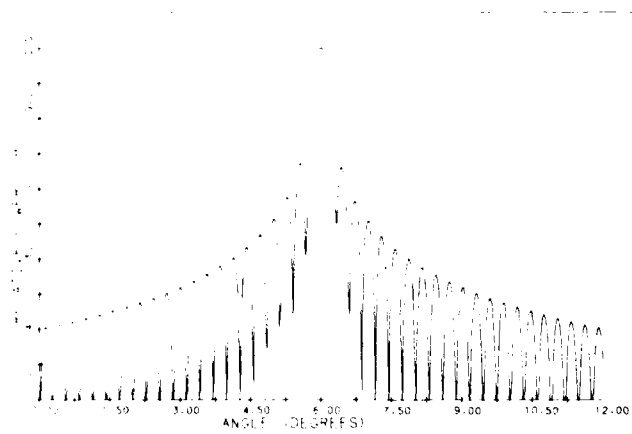
Figure 4. Geometry of a Two Degree of Freedom Lens



(a)



(b)



(c)

Figure 5. Scanned Beam Patterns of a Two Degree of Freedom Lens: (a) 3.0° Beam, (b) 6° Beam, and (c) 6° Beam With Refocusing

3.2 Subarrays

As shown in Reference 2 this lens can form low sidelobe patterns with subarrays of only three elements (seven for a lens that scans in both azimuth and elevation). Since with $L = 200\lambda$ the beamwidth is about 0.3° , the subarray elements must be at 0.3° intervals along the focal arc. Appendix A of Reference 2 shows that when three adjacent subarray elements have relative amplitudes of 0.426, 1.0, and 0.426, the peak sidelobe is -48 dB. Figures 6a and 6b are patterns of subarrays at 0° and $+6^\circ$ for a 200λ diameter lens with $F/L = 1$. In these patterns and all others shown in this report all elements are assumed to have cosine element patterns. Attenuation of $R^{-0.5}$ is assumed between elements within the lens. Patterns are gain referenced to the beam peak of a single on-axis subarray element.

With 0.3° spacing in angle, the distance between subarray elements is about 1.05λ . That spacing will be unacceptable when the mask is inserted, because subarray grating lobes will form on the mask. Therefore, for $F/L = 200\lambda$, we would choose to use a seven-element subarray with 0.15° spacing and amplitude weights of 0.2264, 0.426, 0.8174, 1.00, 0.8174, 0.4260 and 0.2264. In a system that scans in both azimuth and elevation, the subarray will actually be a two-dimensional equilateral triangular lattice of elements. A subarray seven elements across would contain 37 elements. The subarray elements must have both amplitude and phase control: amplitude control for low-sidelobe synthesis; and phase control for beam steering.

3.3 Grating Lobe Analysis

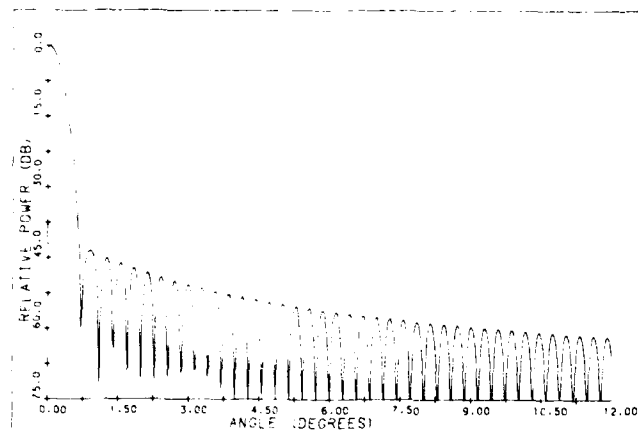
When the phase shift mask is added to the antenna there are three additional grating lobe conditions. Not only must the lens not produce grating lobes on the earth, it must also not produce any on the mask. The latter requirement is much more restrictive since the mask has a greater angular extent (viewed from the lens) than does the earth. Similarly, the mask must not be allowed to produce grating lobes on either the lens or the subarray.

Figure 7 shows the geometry relevant to this problem. We find the width of the mask, L_M , from the requirement that a focused wave (receive case) from $\pm\theta_{\max}$ not spill over the mask edge;

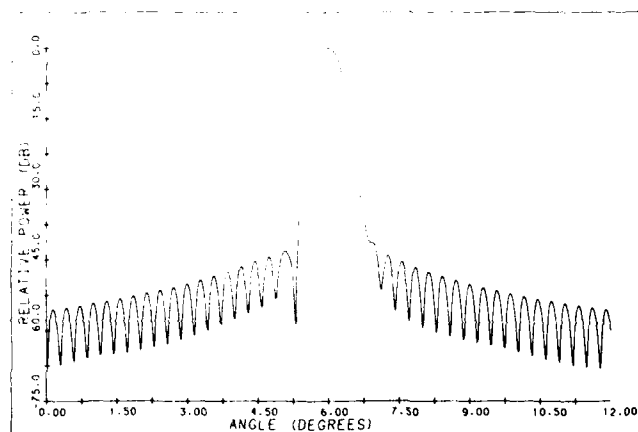
$$L_M \geq DL/F + 2(F-D) \sin \theta_{\max} . \quad (5)$$

The angle of the mask edge from the lens centerpoint is

$$\gamma_{ML} = \tan^{-1} [L_M/2(F-D)] . \quad (6)$$



(a)



(b)

Figure 6. Synthesized Low Sidelobe Patterns Using a Three-Element Feed, $F = L = 200\lambda$: (a) On-axis Pattern, and (b) 6° Scanned Beam

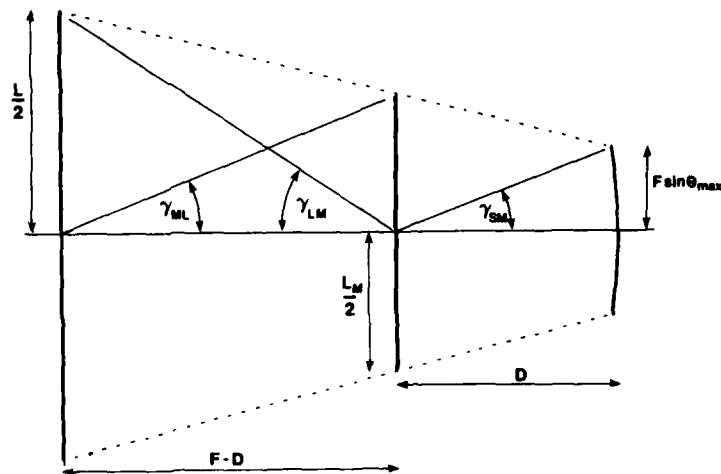


Figure 7. Reference Geometry for Grating Lobe Analysis

The maximum spacing of elements is now found from

$$\lambda/d_L \leq |\sin \gamma_{ML} + \sin \theta_{\max}| \quad (7)$$

Figure 8 shows $d_{L\max}$ as a function of the mask position D for a few choices of F/L . As expected, the closer the mask is to the focal arc, the larger the permissible lens element spacing.

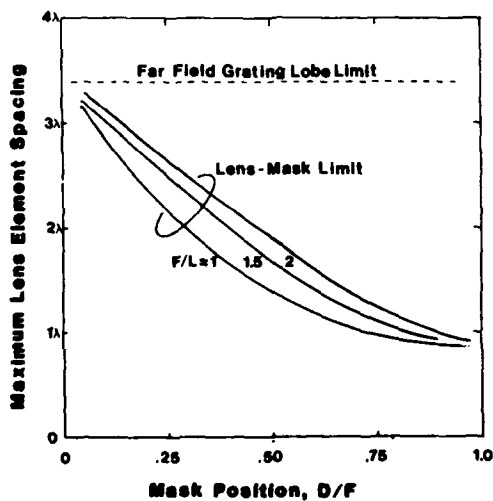


Figure 8. Maximum Lens Element Spacing vs Mask Position

In this antenna the lens elements are passive. The mask elements, on the other hand, contain phase shifters and we would like to have as few of them as possible for reasons of cost. To find out how widely we can space them we refer again to Figure 7. The lens limits the mask element spacing to

$$\lambda/d_M \leq |\sin \gamma_{LM} + \sin \theta_{\max}| \quad (8)$$

where

$$\gamma_{LM} = \tan^{-1} [L/2(F-D)] . \quad (9)$$

The subarray limits d_M to

$$\lambda/d_M \leq |\sin \gamma_{SM} + \sin \theta_{\max}| \quad (10)$$

where

$$\gamma_{SM} = \tan^{-1} [F \sin \theta_{\max}/D] . \quad (11)$$

These two limits are plotted in Figure 9. Figure 10 shows the number of mask elements required for a lens with a circular aperture of 233λ diameter:

$$N_M = \pi [L_M/2d_M]^2 . \quad (12)$$

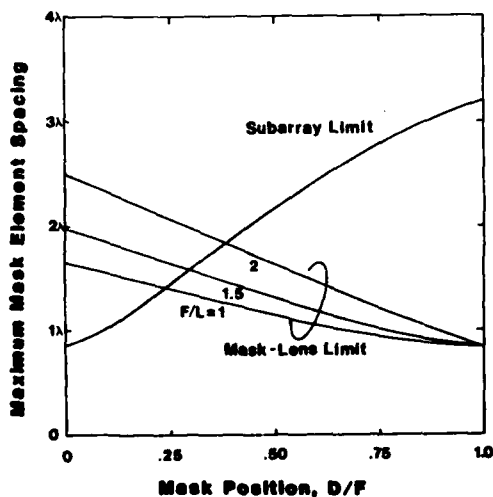


Figure 9. Maximum Mask Element Spacing vs Mask Position

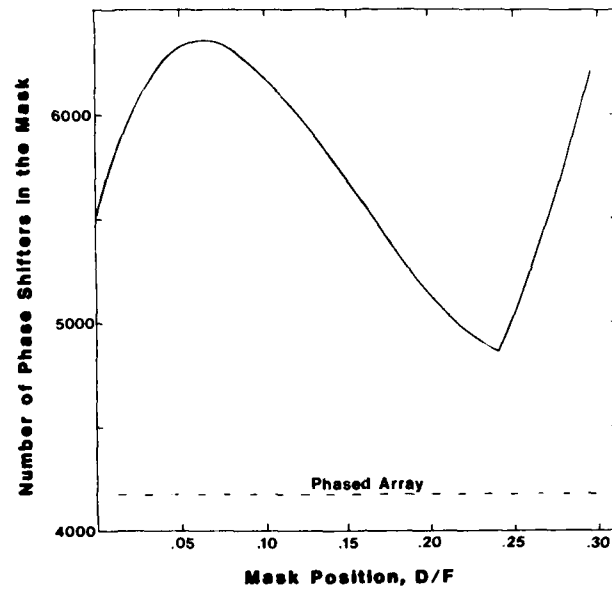


Figure 10. Number of Mask Elements Required for a 233λ Aperture

By comparison, a phased array with the same aperture size would need approximately 4170 elements. The minimum number of mask elements is about 4850. Thus, it is clear that this antenna has no advantage in the ability to steer a single beam. For multiple beams, however, the phased array would need a separate feed network and a separate bank of phase shifters for each beam. The next section shows how the mask can steer multiple beams with only a small increase in the number of its elements.

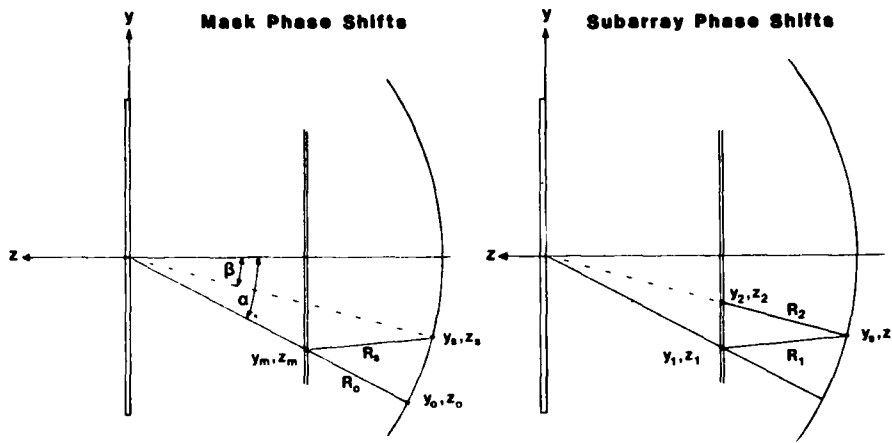


Figure 11. Reference Geometry for Beam Steering:
(a) Mask Steering and (b) Subarray Steering

4. SCANNING CHARACTERISTICS

4.1 Beam Steering Algorithm

A wave incident on the lens from an angle α would normally focus at (y_o, z_o) . $(y_o, z_o) = (-G \sin \alpha, -G \cos \alpha)$. The focal length G is a function of α which equals F only at the points of perfect focus, $\alpha = \pm \beta$.

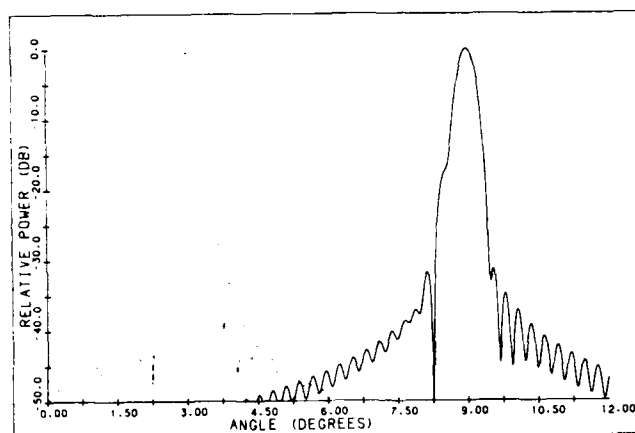
As Figure 11a shows, the mask must redirect the wave so that it focuses at $(y_s, z_s) = (-G(\beta) \sin \beta, -G(\beta) \cos \beta)$. To do so, the mask applies a phase shift of

$$\Psi_m = k (R_o - R_s) \quad (13)$$

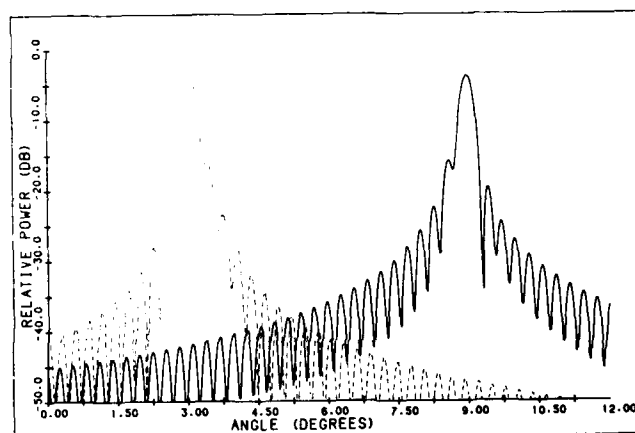
where $k = 2\pi/\lambda$ and

$$R_o = [(y_o - y_m)^2 + (z_o - z_m)^2]^{1/2} \quad (14)$$

$$R_s = [(y_s - y_m)^2 + (z_s - z_m)^2]^{1/2}. \quad (15)$$



(a)



(b)

Figure 12. Scanned Subarray Patterns, $\alpha_s = 6^\circ$, $F = L = 200\lambda$:
 (a) Large Mask-Subarray Separation, $D = F/8$ and
 (b) Small Mask-Subarray Separation, $D = F/16$

We must also apply a phase shift to the subarray to steer it to that part of the mask illuminated by the focusing wave (Figure 11b):

$$\psi_s = k(R_2 - R_1) \quad (16)$$

$$R_1 = [(y_s - y_1)^2 + (z_s - z_1)^2]^{1/2} \quad (17)$$

$$R_2 = [(y_s - y_2)^2 + (z_s - z_2)^2]^{1/2} \quad (18)$$

Note that neither of these phase shift terms is linear. The linear phase shifts that come closest to the correct ψ_m and ψ_s would be found using the first terms of binomial expansions of the square roots in Eqs. (14), (15), (17), and (18). However, because of the small distances between the mask and the subarrays those "paraxial" approximations are inadequate.

4.2 Single Beam Scanning

Figure 12 demonstrates the effectiveness of our beam steering algorithm. The approximate ψ_s and ψ_m are applied to, respectively, the 6° subarray and the mask to steer that beam to 3° and 9° . In Figure 12a the mask is located at $D = F/8$ from the center of the focal arc, and fairly good patterns are maintained at these maximum scan angles. However, with the smaller mask-focal arc separation ($D = F/16$) of Figure 12b, there is considerable degradation in sidelobe levels as well as a loss in gain. The reason for this, shown in Figure 13, is that the mask is illuminated at a very oblique angle by the (transmitting) subarray. The resulting mask and lens amplitude distributions are quite asymmetric.

Clearly, making D large will prevent this effect since it would limit the angle a subarray must scan relative to its own boresight. But that poses a conflict with the need for multiple beams, which will overlap on the mask unless D is small, as illustrated in the following section.

4.3 Multiple Beam Scanning

When several subarrays are required to scan simultaneously, their beams will overlap on the mask if their respective users are close to each other in angle. Figure 14 shows the percentage overlap for two subarrays steered to within α degrees of each other for various D/F ratios, calculated as

$$\% \text{Overlap} = 1 - \sin \alpha (F^2 - DF) / DL \quad (19)$$

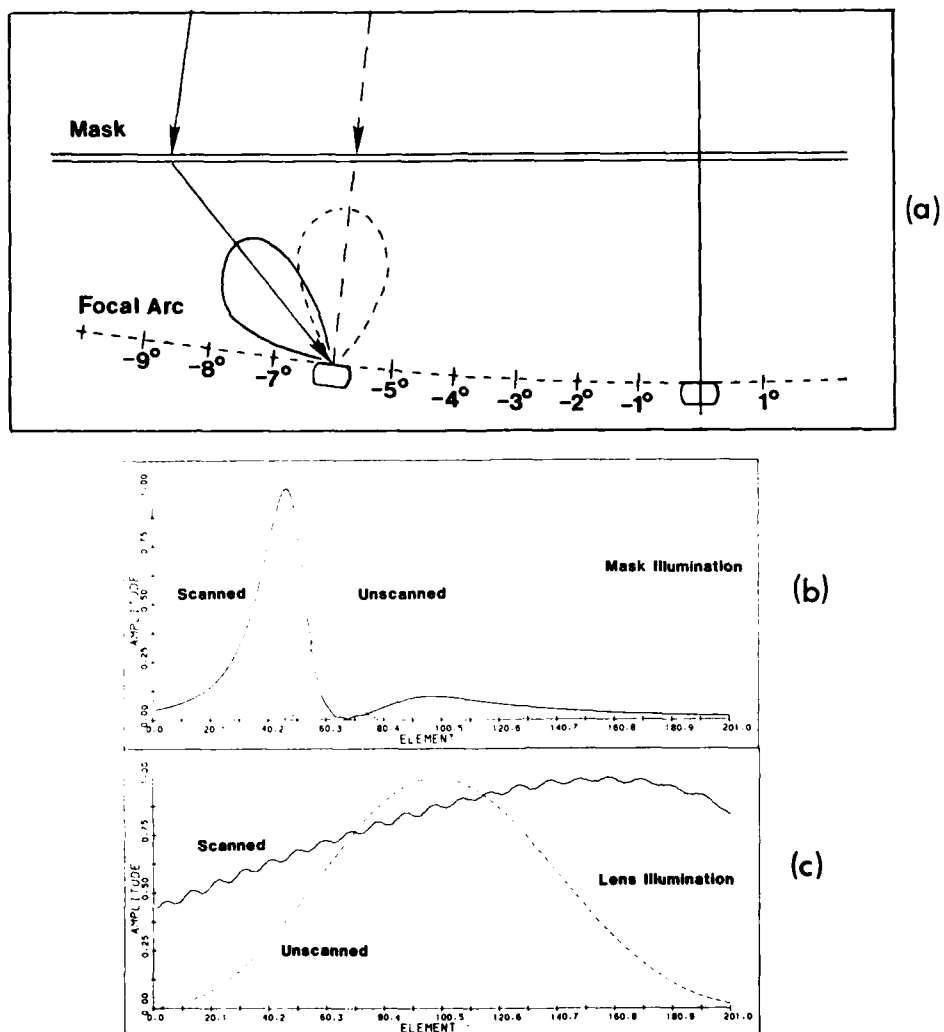


Figure 13. Oblique Mask Illumination by the Subarray, 6° Subarray Scanned to 9° : (a) Geometry, (b) Mask Amplitude Distribution and (c) Lens Amplitude Distribution

By finding the allowable % beam overlap, we will determine the permissible range of D/F .

The minimum separation depends to some extent on how the phase shifters are set in that overlap region. If the mask phases are set properly for one beam, the area available to the other beam is truncated. If the phases in the overlap region are randomized, that much mask area is denied to both beams, with a consequent

reduction in gain. The best approach is to find the point on the mask where the amplitude due to each beam is the same, or the crossover point, and set the phases on either side of that point to satisfy the nearest subarray. That point is very nearly halfway between the peaks of each beam's amplitude distribution on the mask, which is assumed in the following simulations. The allocation of the mask to adjacent subarrays is illustrated in Figure 15a.

Figures 15b and 15c show the effect on the unsteered 6° subarray when the 0° subarray is steered to various angles, for $D/F = 8$ and $D = F/16$, respectively. In the $D/F = 8$ case, the patterns are acceptable until the two beams are steered to within 7° of each other. For $D/F = 16$, on the other hand, they may come to within 3.5° , which implies that adjacent beams may not overlap by more than 10 percent on the mask (see Figure 14).

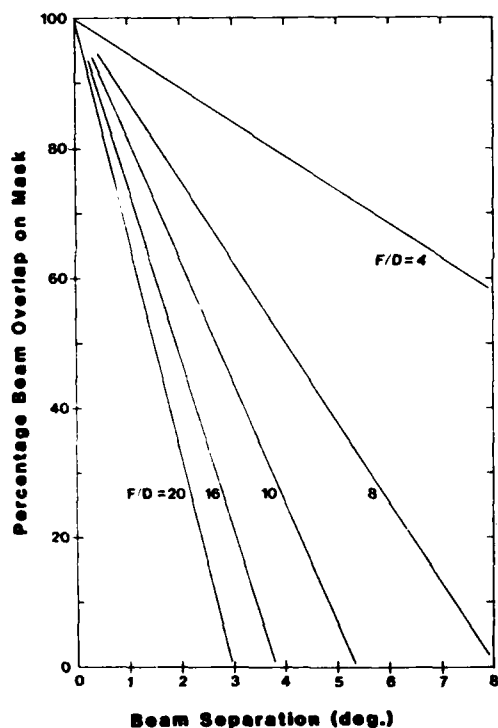


Figure 14. Percentage Mask Overlap by Adjacent Subarrays

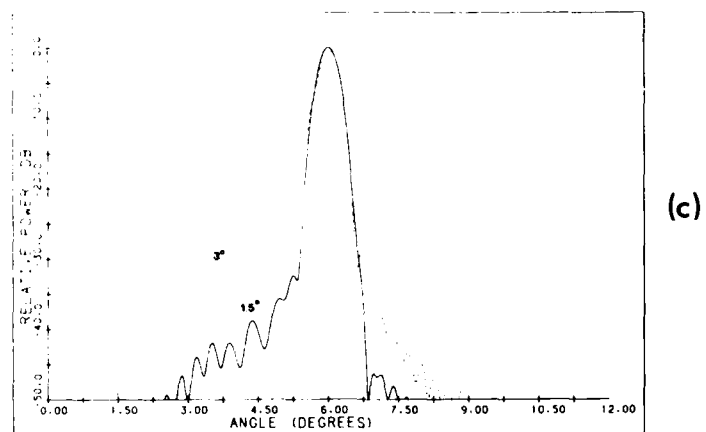
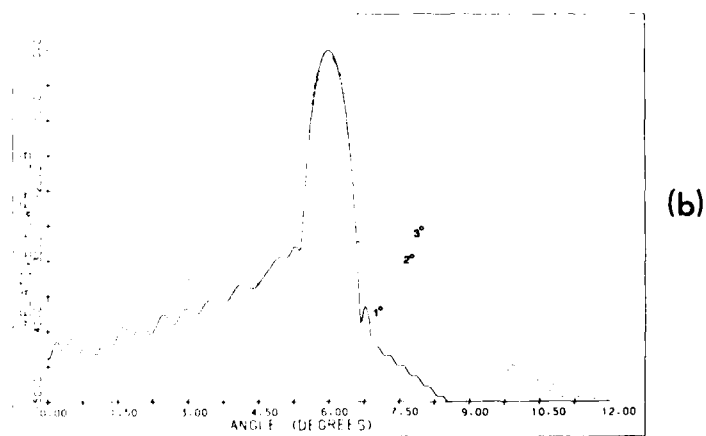
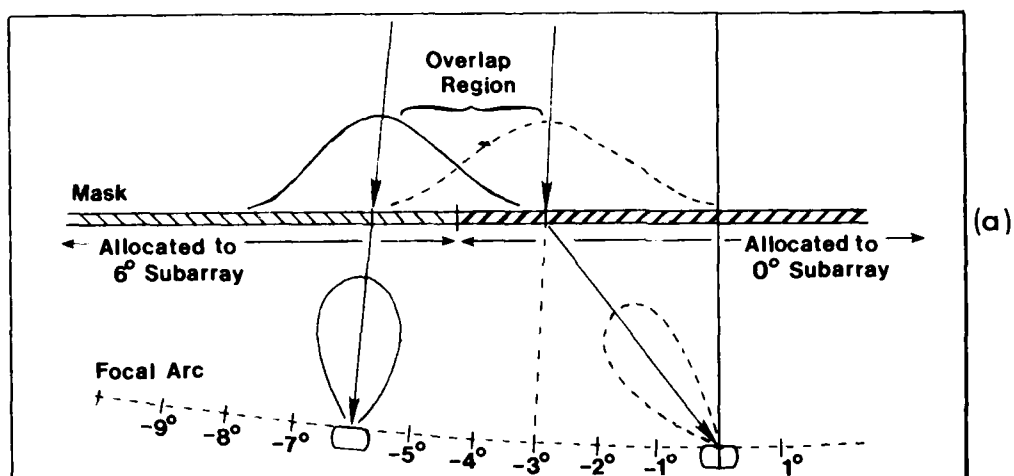


Figure 15. Effect on 6° Subarray's Pattern Due to Scanning of 0° Subarray, $F = L = 200\lambda$, 7-Element Subarray: (a) Allocation of Mask Area to Overlapping Beams, (b) $D = F/8$, and (c) $D = F/16$

Figure 16 is the opposite case—the 0° subarray remains at broadside scan while the 6° subarray is steered. Here we see not only the effects of mask overlap, but also the previously mentioned beam steering effects. For the small mask displacement, $D = F/16$ the overlap effects are less, but steering effects are greater since the subarray must scan to wider angles. It is interesting to note that the decrease in gain is nearly the same for the 3° scan in both Figures 16a and 16b even though its cause is different.

There are essentially two possible ways around this problem: (1) increase the focal length; or (2) use more subarrays. A larger focal length causes the beams to overlap less for a given D/F ratio. Figure 17 shows the improvement gained by increasing the lens focal length to twice its length ($F/L = 2$). Unfortunately, that requires an increase in the mask diameter to 135λ [see Eq. (5)], and a consequent increase to 12,600 phase shifters.

Alternatively, we could increase the number of subarrays. The simulations discussed thus far have used a configuration of three subarrays, corresponding to seven for a three-dimensional system (an equilateral lattice three subarrays across). With five subarrays across, the 3D system would have a total of 19. Each of those 19 would have to cover about a 3.6° solid angle, or $\pm 1.8^\circ$ in all directions around their unsteered angles. Figure 18 indicates that spacing would be adequate. It shows the patterns of a subarray located at -4° , with adjacent subarrays at 0° and -8° . Because the -4° subarray must only scan the region from 2° to 6° , there is little degradation due to the beam steering, although there are still overlap effects, indicated by the higher near-in sidelobes. Because increasing the number of subarrays does nothing to eliminate the overlap, there is no improvement between Figure 18b and Figure 15c.

If each subarray is an equilateral lattice seven elements across, or a total of 37 elements, the total number of focal elements increases from 259 to 703 with 19 subarrays instead of seven. This seems a far better alternative than increasing the F/L ratio to two, which trebles the number of mask elements.

In conclusion, the antenna design we would recommend based on the foregoing results would use a 200-wavelength diameter lens, for a beamwidth of 0.3° , and F/L ratio equal to one. The mask would be located at $F/16$ from the center of the focal arc, which would contain an equilateral lattice of subarrays, five subarrays across, for a total of 19. Each subarray would contain 39 elements in an equilateral lattice seven elements across. Variable phase control over the subarray elements is required, but only fixed amplitude control. Phase control only is used at the mask.

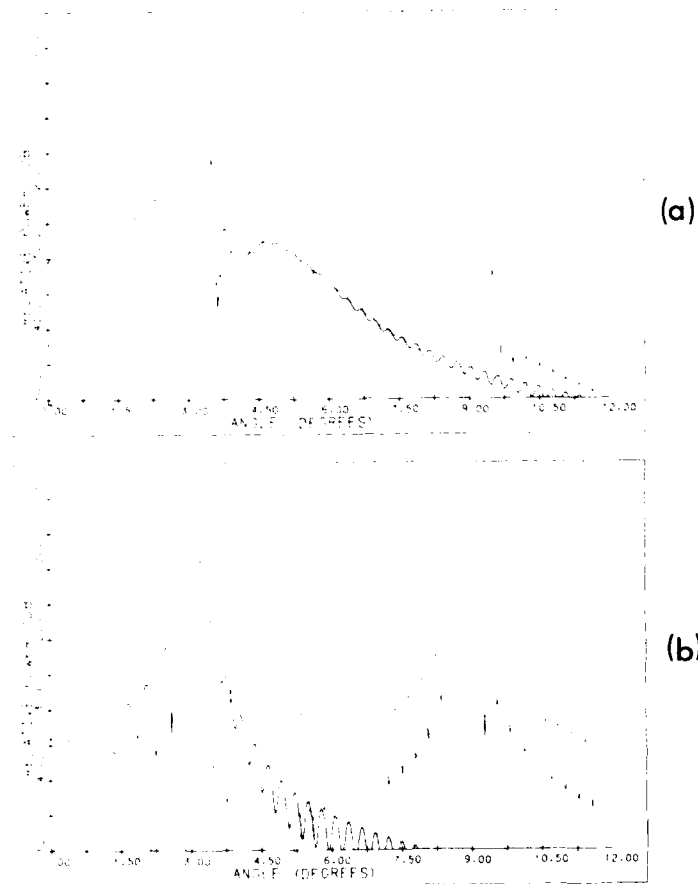
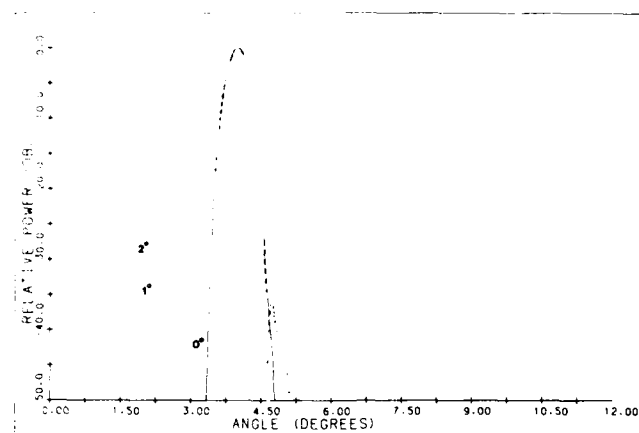
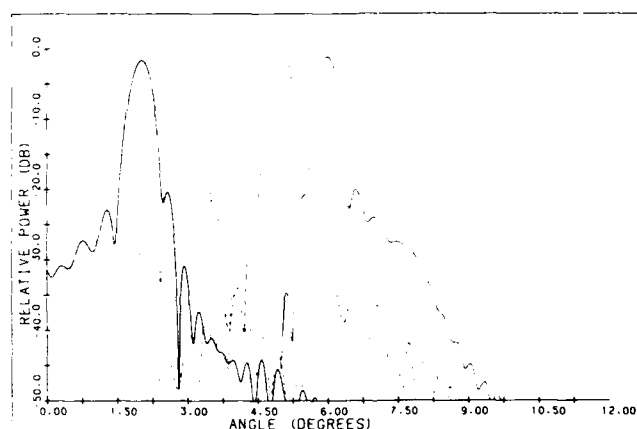


Figure 16. Scanned Patterns of 6° Subarray With 0° Subarray
Unscanned, $F = L = 200\lambda$, 7-Element Subarray: (a) $D = F/8$,
and (b) $D = F/16$



(a)



(b)

Figure 18. Scanned Patterns With Short Focal Length and Smaller Subarray Spacing, $F = L = 200\lambda$, $D = F/16$:
(a) 0° Subarray Scanned and (b) 4° Subarray Scanned

5. CONCLUSIONS

In conclusion, this antenna architecture does allow scanning of multiple, independent beams. Pattern quality is reasonable provided that no two users within 1.5° of each other are to be served simultaneously. A system capable of providing full earth coverage with a 0.5° beamwidth will contain less than 5000 phase shifters in the mask—only 20 percent more than required for a single-beam phased array for the same coverage region.

In this first look at a new concept, we have tried to keep the system geometry as simple as possible for reasons of being able to interpret the results. It is quite possible that other variations will yield better results. For example, if the "mask" were curved concave to the focal arc, skewing of the subarray beams would not be such a problem. Also, it may be possible to locate the subarrays behind the focal surface, and use the mask phase shifts for refocusing as well as steering. Indeed, it is quite possible that varying the shape of the mask surfaces and the length of lines connecting its two faces will yield a lens with still better off-axis focusing properties. These are all potential areas of further study.

MISSION of Rome Air Development Center

RADC plans and executes research, development, test and selected acquisition programs in support of Command, Control, Communications and Intelligence (C³I) activities. Technical and engineering support within areas of competence is provided to ESD Program Offices (POs) and other ESD elements to perform effective acquisition of C³I systems. The areas of technical competence include communications, command and control, battle management, information processing, surveillance sensors, intelligence data collection and handling, solid state sciences, electromagnetics, and propagation, and electronic, maintainability, and compatibility.

Printed by
United States Air Force
Hanscom AFB, Mass. 01731

END

FILMED



DTIC